https://doi.org/10.30799/jnst.192.19050101 J. Nanosci. Tech. - Volume 5 Issue 1 (2019) 580–583

ISSN: 2455-0191

Share Your Innovations through JACS Directory

Journal of Nanoscience and Technology

Visit Journal at http://www.jacsdirectory.com/jnst

Synthesis, Characterization of α-Al_2O_3 Nanoparticles and Its Application in Decolorization of Methyl Orange Azo Dye in the Presence of UV Light

Vijaya P. Dhawale[1,*], Datta J. Late[2], Satish D. Kulkarni[3]

[1]Post Graduate Department of Physics, New Arts Commerce and Science College Parner, Ahmednagar – 412 210, Maharashtra, India.
[2]Physical and Materials Chemistry Division, CSIR-National Chemical Laboratory, Dr. Homi Babha Road, Pune – 411 008, Maharashtra, India.
[3]Post Graduate Department of Environmental Science, New Arts Commerce and Science College, Ahmednagar – 414 001, Maharashtra, India.

ARTICLE DETAILS

Article history:
Received 05 December 2018
Accepted 23 December 2018
Available online 05 January 2019

Keywords:
Sol-Gel Method
α-Al_2O_3 Nanoparticles
Azo Dye
Decolorization

ABSTRACT

Present study deals with the sol-gel synthesis and application of α-Al_2O_3 nanoparticles (alumina) to decolorize the azo anionic dye methyl orange (MO). α-Al_2O_3 nanoparticles were successfully synthesized using aluminium oxide, 25% ammonia and polyvinyl alcohol (PVA) were used as low cost raw materials. The properties of synthesized nanoparticles were investigated by using UV-visible spectroscopy, XRD, FTIR, SEM, EDAX, Raman spectroscopy and TEM. From UV–visible spectra, band gap was calculated and it was found to be 3.31 eV. Average crystal size of α-Al_2O_3 nanoparticles from XRD peaks found to be 25 nm having rhombohedral structure. FTIR spectra reveals that functional groups (O-Al-O) are present. SEM image shows distribution pattern of α-Al_2O_3 nanoparticles. Chemical composition of α-Al_2O_3 nanoparticles was confirmed from EDAX spectroscopy measurement. Raman spectra showed crystalline nature of α-Al_2O_3 nanoparticles. The effect of concentration and pH of dye, dosage of nano adsorbent and contact time were studied. The systematic study shows that, successful color removal of methyl orange dye up to 54% in three hours contact time of pH 4. Hence α-Al_2O_3 nanoparticles can be used for dye removal from waste water. Industrialization of this technique will be cost effective way to decolorize the textile dye present in water system.

---

1. Introduction

Azo dyes represent the largest class of dyes, characterized by at least one azo group (-N=N-) with one or more aromatic groups. Most of these dyes are toxic and potentially carcinogenic in nature. Many industries like textiles, leather, paints, varnishes, pharmaceuticals, plastic and cosmetics etc. use dyes to colour their products. Consequently, the wastewater effluents are highly coloured, toxic and non-biodegradable. These dyes promote eutrophication and adversely affect the environment. About 100,000 dyes are commercially available [1] and more than 700,000 tons of dyes are synthesized worldwide annually for textile industry. An unfortunate side effect of their widespread use is the fact that up to 12% of these dyes are washed during the dyeing process, and that approximately 20% of this wastage enters the aquatic environment. Due to their complex structure, stability and synthetic origin, dyes are not easily biodegradable. Some dyes are reported to cause allergy, dermatitis, skin irritation, cancer and mutations in human being [2]. Therefore, the treatment of effluents containing dyes is one of the challenging problems all over the world.

Various methods such as adsorption, coagulation, biodegradation, advanced oxidation process (AOP) and the membrane process have been developed to degrade and remove these carcinogenic dyes from the wastewater. At present physical, chemical and biological methods are used as a treatment process for removal of dyes from wastewater. Among these methods, advanced oxidation process (AOP) have been reported to be effective for the degradation of soluble organic pollutants from wastewaters and soils as they provide an almost total degradation. As a result, an environmental-friendly technology has become a necessary for removal of dye from wastewater. All these processes have some advantages or disadvantages over the other method. Among these methods, adsorption is a conventional technology for dye removal with very high efficiency and simple process. Thus, application of nanoparticles as adsorbents has come up as an interesting area of research because of their small particle size and high surface area. The active sites are also more and capable of interacting with pollutant species [3].

Methyl orange (MO), a basic (anionic) water soluble dye, is most widely used for coloring purposes. It is widely used worldwide in textile, paper, food, printing and pharmaceutical industries. The effluents from these industries are a major source of environmental pollution. Not only water bodies become coloured, but it also affects growth of aquatic organisms by blocking the penetration of sunlight and decreasing the dissolved oxygen capacity of water. Thus, MO is selected as a model dying pollutant to evaluate the catalytic activity of the aluminium oxide nanoparticles (AONP). Aluminium oxide nanoparticles are prepared by using sol-gel method [4]. The material of high purity can be prepared by this method. Polyvinyl alcohol (PVA) is used here as a capping agent to cap the particles, providing them stability [5]. In addition, polymer additives such as poly (vinyl) alcohol (PVA) or sodium citrate may be added as surfactant to keep the formed nanoparticles both dispersed and spherical in shape [6]. In the present study aluminium oxide nanoparticles are used as adsorptive removal of MO from aqueous medium.

2. Experimental Methods

2.1 Synthesis of Aluminium Oxide Nanoparticles

The nanoparticles were prepared by the sol-gel technology. All chemicals used were analytical grade. Aluminium chloride, $AlCl_3$ (Molychem), 25% NH_3 solution (Qualigen Fine Chemicals) and polyvinyl alcohol (PVA) (Modern Industries) were used as raw materials for the synthesis of aluminium oxide nanoparticles. 0.1 M alcoholic $AlCl_3$ solution was prepared, followed by addition of 25% ammonia solution. The resulting solution turned to a white solution. This was followed by the addition of PVA (0.5 M). The solution was stirred continuously using a magnetic stirrer until it became a transparent sticky gel. The gel was allowed to mature for 24 hours at room temperature. The resultant gel was heat treated at 100 °C for 24 hours which led to the formation of light weight porous materials due to the enormous gas evolution. The dried gel was, then calcined at 1200 °C for 4 hours and finally, the calcined powders were crushed using mortar and pestle to get the fine homogeneous dense powder [5].

---

*Corresponding Author:vijaya.dhawale2009@gmail.com(Vijaya P. Dhawale)

https://doi.org/10.30799/jnst.192.19050101

Cite this Article as: Vijaya P. Dhawale, Datta J. Late, Satish D. Kulkarni, Synthesis, characterization of α-Al_2O_3 nanoparticles and its application in decolorization of methyl orange azo dye in the presence of UV light, J. Nanosci. Tech. 5(1) (2019) 580–583.

2.2 Photocatalytic Degradation Studies

Photocatalytic activities of the as-synthesized powder were evaluated by decolorization of methyl orange dye in aqueous solution. The experiments were carried out in the presence of UV light irradiation without any adsorbent (blank) and in the presence of UV light with adsorbent. The photocatalytic reactor consists of a glass chamber with an inlet tube for provision of dye solution purging during photocatalysis and outlet tube for the collection of samples. Distilled water was used to prepare all stock solution and stored in dark bottles. From a stock solution of 1000 mg/L of the dye, different concentrations were made. Reaction was set up by adding different dose of the as-synthesized aluminium oxide nanopowder (50, 80, 100 mg) into 1000 mL of MO solution of concentration (10 mg/L) in the glass chamber. The solution was magnetically stirred in with and without nanoparticle addition into dye solution for 180 minute to obtain adsorption equilibrium after irradiating the UV light sources in the chamber of the reactor. Sample was withdrawn at 30 minute time interval over contact time for 180 minute. The solution was filtered through Whatman filter paper to remove the nanoparticles before measuring absorbance. The absorbance of sample was measured at 466 nm using visible double beam spectrophotometer (Systronics, Model 1203). For quantitative analysis percentage degradation of MO dye was calculated using the following formula,

$$\%\ \text{decolourisation} = \frac{(A_o - A_t)}{A_o}\ \text{X}100$$

where A_o is absorbance of dye at initial stage, A_t is absorbance of dye at time t.

$$q_e = \frac{(A_o - A_t)}{W} X\ V$$

where, q_e is the amount of dye adsorbed at the time of equilibrium (mg/g), Ao and At are initial and final concentration of dye (mg/L), V (L) is the volume of sample, and W (g) is the mass of adsorbent [7].

3. Results and Discussion

3.1 Characterization

3.1.1 UV-Visible Spectroscopy

The UV absorption ability of α-Al_2O_3 is related with band gap energy. Band gap energy of α-Al_2O_3 nanoparticle is calculated from UV –Vis absorption spectrum. The spectrum shows two absorption peaks at 205 nm and 265 nm in the UV region as shown in Fig. 1. The photo excitation of electron from valence band gives band gap energy (E_g). The band gap energy (E_g) was estimated by the Wood and Tauc method, according to the following equation, $(h\nu\alpha) = (h\nu - E_g)^n$, where, 'α' is the absorption coefficient, 'h' is Planck's constant, 'ν' is the frequency, 'E_g' is absorption band gap energy and 'n' is a constant associated to the different type of electronic transitions (n=1/2, 2, 3/2 or 3 for direct allowed, indirect allowed, direct forbidden, indirect forbidden transitions respectively). E_g value for the Al_2O_3 nanoparticles is 3.31 eV. These results are in good agreement with those previously reported by Varghese et al. [5] and, Farahmandjou and Golabiyan [8].

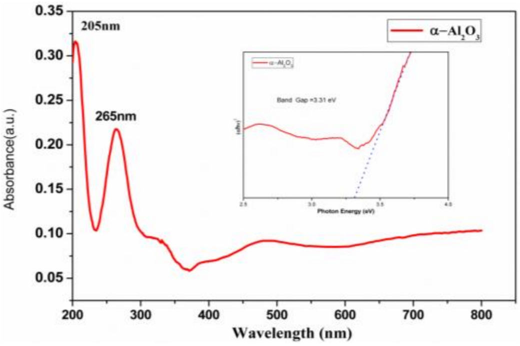

Fig. 1 Typical UV-vis spectra of α- Al_2O_3 nanoparticles. The inset shows the Wood and Tauc plot used to find out band gap of α-Al_2O_3

3.1.2 X-Ray Diffraction Patterns (XRD)

The peaks in the XRD pattern significantly supported formation of nano sized α-Al_2O_3 nanoparticles from JCPDS file (71-1683) having rhombohedral structure. Eleven reflections were observed at 2θ angles around 25° (012), 35° (104), 38° (110), 43° (113), 52° (024), 57° (116), 60° (122), 61° (018), 66° (214), 68° (300) and 70° (119). Average crystallite size was calculated from all peaks and was found to be 25 nm, whereas, the lattice constant 0.614 using Debye Scherrer formula, D=0.9λ/βcosθ where, 'D' is the crystalline size, 'λ' is the wavelength of CuKα radiation, 'β' is full width half maximum (FWHM) of the diffraction peak and 'θ' is Bragg's angle of X ray diffraction peak (Fig. 2a). Similar results have been obtained by others [9]. XRD analysis exhibits that the most stable phase, α-Al_2O_3 was obtained at 1200° C. The observations reported by Hyuk-Joon et al. [10], noted that completion of the most stable phase of α- alumina occurs at this temperature. During thermal treatment, stable α- Al_2O_3 phase can be obtained through the following series of phase transformation before conversion to α- Al_2O_3:

$$\text{Hydrous alumina} \longrightarrow \text{bohemite} \longrightarrow \gamma \longrightarrow \delta \longrightarrow \theta \longrightarrow \alpha$$

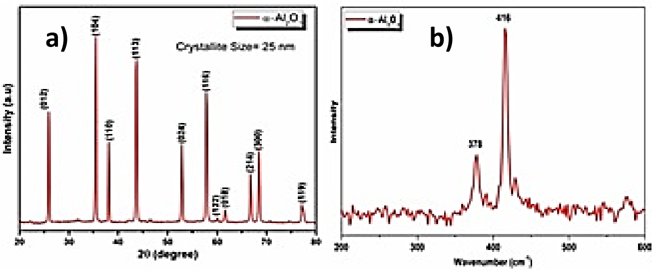

Fig. 2 α-Al_2O_3 nanoparticles (a) XRD pattern and (b) typical Raman Spectra

3.1.3 Fourier Transform Infrared Spectroscopy (FTIR)

The infrared spectrum (FTIR) of the synthesized α-Al_2O_3 nanoparticles was in the range of 400-4000 cm^{-1} wave number which identify the chemical as well as functional groups in the compound. The FTIR spectra revealed that, there are 418.55, 432.05, 445.56, 455.20, 489.92, 507.28, 570.93, 588.29, 607.58, 630.72, 696.30 cm^{-1} (O-Al-O) functional groups (Fig. 3). An intense band centered 3500 cm^{-1} and other around 1600 cm^{-1} was assigned to O-H stretching and bending modes of water or alcohol respectively. The wide band appearing between 500 cm^{-1} and 900 cm^{-1} corresponds to the vibrational frequencies of co-ordinate O-Al-O bond. The wide band is divided into two peaks. The peaks in the region 500 – 750 cm^{-1} were assigned ν –AlO_6 and the other at 800 cm^{-1} was assigned to ν – AlO_4 in nano Al_2O_3 [11]. There are some wide and high peaks of Al–O stretching (AlO_4 or AlO_6 vibration) in the range of 500 – 1000 cm^{-1} (507.28, 570.93, 588.29, 607.58, 630.72, 696.30, 756.10, 813.96, 844.82) that relates to the transitional phases of alumina and stable phase of alumina (alpha) [12].

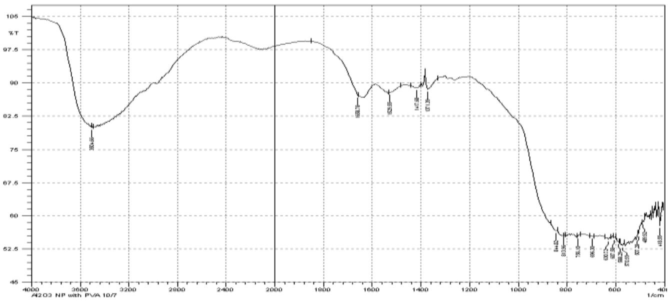

Fig. 3 FTIR of α-Al_2O_3 nanoparticles

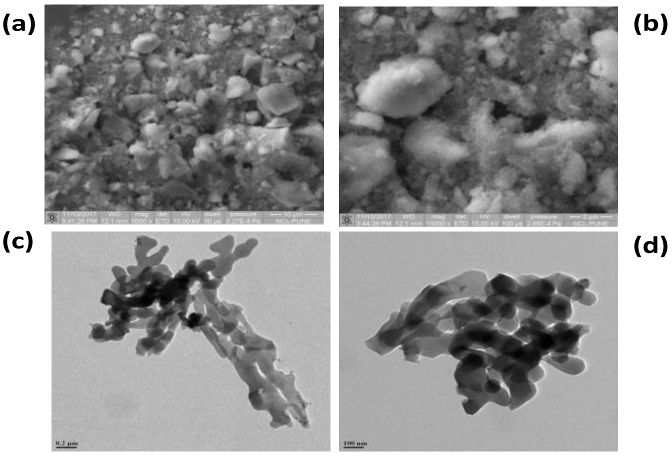

Fig. 4 α-Al_2O_3 nanoparticles (a,b) SEM images and (c,d) TEM images

https://doi.org/10.30799/jnst.192.19050101

Cite this Article as: Vijaya P. Dhawale, Datta J. Late, Satish D. Kulkarni, Synthesis, characterization of α-Al_2O_3 nanoparticles and its application in decolorization of methyl orange azo dye in the presence of UV light, J. Nanosci. Tech. 5(1) (2019) 580–583.

3.1.4 Scanning Electron Microscopy (SEM)

SEM image gives the distribution pattern and size of the nanoparticles (Fig. 4a and b). The surface morphology of the alumina nanoparticles was obtained through SEM. The SEM micrograph shows irrergular shape of particles and spongue like structure.

3.1.5 EDAX

EDAX spectrum shows the chemical composition of Al_2O_3 nanoparticles analysed by EDAX. Result indicates the presence of Al and O as the main elements. This analysis is important because it confirms that α-Al_2O_3 nanoparticles are effectively composed of Al and O with no contamination indication which confirms the formation of alumina nanoparticles.

3.1.6 Raman Spectroscopy

Raman spectra shows characteristics peaks at 378 cm^{-1} and 416 cm^{-1} (Fig. 2b). The results obtained are in accordance with previous works. Cava et al. [13] reported that transformation of all pure alumina into the single α-phase was observed starting from 1050 °C, the sharp peaks of the α-phase indicate the relatively large grain sizes and well-defined long-range order in corundum. Peaks due to γ- Al_2O_3 disappear when the temperature is higher to 1050 °C, forming α-Al_2O_3 [13]. The powders do not present any impurities, due to incomplete transformations of any intermediate phases, as θ and δ, as it happens in conventional methods of processing [14]. Usually, by means of traditional methods of synthesis, any aluminum oxide or hydroxide only form α- Al_2O_3 when the material is fired upto 1200 °C [15].

3.1.7 Transmission Electron Microscopy (TEM)

The transmission electron microscope (TEM) analysis was carried out to confirm the actual size of the particles, their growth pattern and distribution of the crystallites. Fig. 4c and d show the TEM image of alumina prepared by sol–gel method. Figure shows the as-synthesized TEM image of α-Al_2O_3 nanoparticles with some agglomeration. Lin et.al. had reported that drying of the sol invariably leads to the agglomeration, since the residual salts present in the sol forms solid bridges between particles as the water evaporates. Besides that, particle size and shape of the α-alumina are determined by crystal structure of original hydroxide and series of phase transformations that occur during calcinations [16].

3.2 Photocatalytic Degradation Studies

3.2.1 Effect of pH

The pH of dye solution plays an important role in the whole adsorption process. In this study, MO dye concentration (10 mg), α-Al_2O_3 nanoparticles dosage (100 mg) was kept constant and pH of dye varied between 2 to 8 at room temperature. Fig. 5a shows % dye removal at different pH of dye solutions. It also shows higher rate (50%) of MO dye removal at pH 4 and minimum removal (20%) of MO dye was found at pH 6. Monash and Pugazhenthi [17] reported the same trend for the adsorption of crystal violet dye on calcinied and uncalcinied mixed clay adsorbents. It is reported that, the zero point surface charge (zpc) of metal oxides play important role in the adsorption at different pH. The surface charge of Al_2O_3 nanoparticles are strongly affected by the aqueous pH conditions. pHzpc facilitates in predicting the surface behaviour of adsorbent materials. The surface charge is positive at pH < pHzpc, neutral at pHzpc and negative at pH > pHzpc. The pHzpc of the Al_2O_3 nanoparticles was found to be 7.4.

At pH 7.4, the net surface charge of adsorbent surface is zero and it becomes electrically neutral whereas at pH > pHzpc, in basic medium, the adsorbent surface becomes negatively charged due to deprotonation thus the adsorption of anionic dye ions get decreased due to Coulomb repulsive forces. In acidic pH condition, when pH < pHzpc, the adsorbent surface is charged positively and leads a higher adsorption of anionic dye due to Coulomb attractive forces. Hence pH of 4.0 was taken as optimum pH for which the adsorbent efficiency for the colour removal of anionic dye is a maximum upto 50% with an initial dye concentration 10 mg/L and Al_2O_3 nanoadsorbent dose 100 mg [18, 19]. The result indicate that the adsorption capacity has decreased with increasing pH. Further, at a fixed pH of 4.0 and 10 mg MO dye concentration, the effect of variation of Al_2O_3 nanoparticles dosage study was carried out. The results are shown in Fig. 5b. It was observed that, percentage of colour removal was 50% for 100 mg Al_2O_3 nanoparticles dose. When Al_2O_3 nanoparticles dose was doubled (200 mg) the percentage of colour removal of dye remains nearly constant. This may be due to the fact that as the Al_2O_3 nanoparticles dose was increased, the number of active sites on the adsorbent surface and the exposed surface area also increases but when the dose of adsorbent increases above the optimum value, the percentage removal rate decreases due to interception of the light by the suspension [20]. Also excess dose of adsorbent prevent the illumination, $^{\cdot}$OH radical, primary oxidant in the photocatalytic system decreased and the efficiency of the colour removal reduced accordingly. Furthermore, the increase of nanoparticle adsorbent dosage beyond the optimum may result in the agglomeration of nanoparticles, hence more adsorbent surface become unavailable for photo absorption and percentage of colour removal rate of adsorbent decreases [21].

3.2.2 Effect of Adsorbent Dose

The use of nanoadsorbent increases surface area of the adsorbent which can lead to more degradation of dye molecules. To investigate the effect of adsorbent dose on the colour removal of dye, experiments were conducted with α-Al_2O_3 nanoadsorbent dose 50 to 100 mg in 1000 mL dye solution at room temperature. It was found that with increase in adsorbent dose, percent degradation of dye molecules increases. Maximum 37% colour removal of dye occurred at 100 mg α-Al_2O_3 nanoadsorbent dose because of increased surface area of nanoparticles which provides more active sites for binding. The variation of % dye removal with respect to α-Al_2O_3 nano adsorbent dose are shown in Fig. 5c.

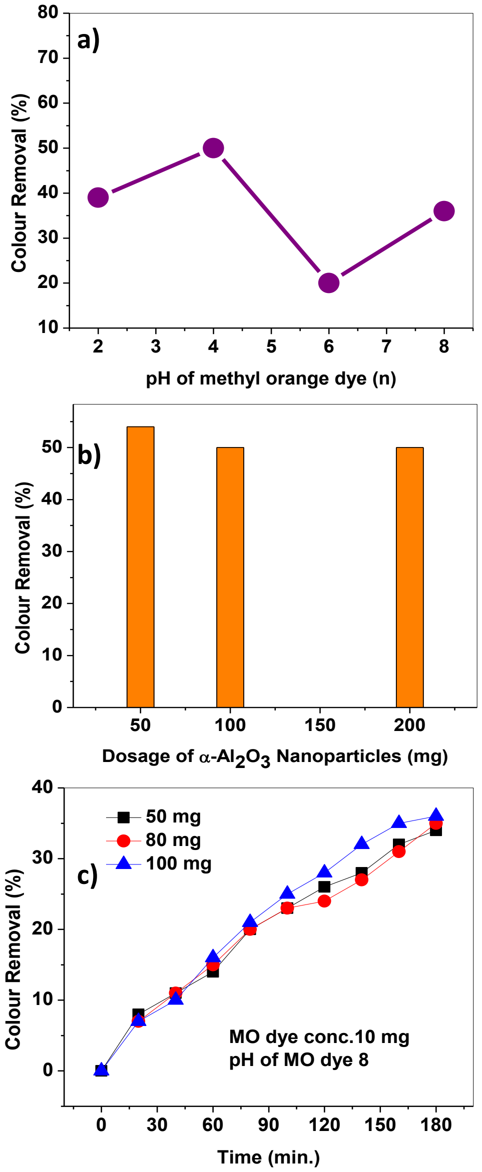

Fig. 5 (a) Variation of % colour removal with pH, (b) Variation of % colour removal with nanoadsorbent dosage and (c) the variation of % colour removal with different α-Al_2O_3 nanoparticles dosage

An attempt was made to enhance % colour removal as a function of nanoadsorbent dose in a solution of pH 4 and pH 8 (Fig. 5b and c). It was found that a fixed methyl orange dye concentration (10 mg) and fixed Al_2O_3 nanoadsorbent dose (100 mg), maximum percentage of dye removal was 50% and 37% for pH 4 and pH 8 respectively. A slower rate of colour removal of dye was attributed to higher molecular weight and structural complexity of the dyes [22].

https://doi.org/10.30799/jnst.192.19050101

Cite this Article as: Vijaya P. Dhawale, Datta J. Late, Satish D. Kulkarni, Synthesis, characterization of α-Al_2O_3 nanoparticles and its application in decolorization of methyl orange azo dye in the presence of UV light, J. Nanosci. Tech. 5(1) (2019) 580–583.

3.2.3 Effect of Initial Dye Concentration

The initial concentration of dye in a given photocatalytic reaction is also another factor which needs to be taken into account. It was found that percent degradation decreases with increasing amount of dye concentration, while keeping a fixed amount of catalyst [23].

3.2.4 Effect of Contact Time

Effect of contact time was studied in the batch mode at methyl orange dye concentration (10 mg/L). The average amount of dye adsorbed (%q_e) in batch experiment was found to be 226.05 mg/g after three hours (Table 1). Result suggests that the adsorption capacity of dyes increases with increasing contact time. The rate of dye removal is initially high due to high concentration gradient and more availability of adsorption sites. The rapid transport of dye molecules from aqueous solutions to the bulk makes the adsorption fast. Surface of Al_2O_3 nanoparticles is charged and net charge at the surface at a particular pH governs adsorptive removal of dye from the solution. The variation of % colour removal with respect to contact time are shown in Fig. 5c.

Table 1 Amount of dye adsorbed (%qe) in batch experiment for concentration of methyl orange dye =10 mg/L

pH of methyl orange dye	Dosage of alumina nanoadsorbent	Amount of dye adsorbed in batch experiment after 3 hours
8	50	391.8
8	80	240.8
8	100	210.8
2	100	166.0
4	100	221.1
6	100	85.4
8	100	210.8
4	50	460.3
4	100	166.0
4	200	107.5
Total Amount of dye adsorbed in batch experiment after 3 hours		2260.5
Average Amount of dye adsorbed in batch experiment after 3 hours		226.05

4. Conclusion

Aluminium oxide nanoparticles (α-Al_2O_3) were successfully synthesized by sol-gel method and the average crystal size was found to be 25 nm having rhombohedral structure from XRD technique. Band gap is 3.31 eV obtained from UV–visible spectra. FTIR spectra shows the (O-Al-O) functional groups thereby indicate formation of aluminium oxide nanoparticles (α-Al_2O_3). X-Ray diffraction patterns confirm the formation of α-Al_2O_3 nanoparticles. The formation of aluminium oxide nanoparticles (α-Al_2O_3) was validated from Raman spectra, SEM, EDAX and TEM analysis. Photo degradation study shows that MO dye can be successfully removed from the aqueous solution by adsorption on aluminium oxide nanoparticles (α-Al_2O_3). It can be effective, reliable and economically used for controlling water pollution due to dyes. The batch adsorption experiments shows that adsorption of MO dye over aluminium oxide nanoparticles (α-Al_2O_3) is dependent on pH, amount of adsorbent, initial dye concentration and contact time. pH of the dye plays important role in colour removal process. At pH 4 and 10 mg concentration of methyl orange dye, maximum colour removal was obtained 50% when aluminium oxide nanoparticles (α-Al_2O_3) dose was 100 mg. So the aluminium oxide nanoadsorbent (α-Al_2O_3) used in this study seems to be very promising for the application in waste water treatment and focus the attention on techniques leading to complete removal of dyes. The present work opens new avenue for the next generation.

Acknowledgement

Smt. Dhawale V. P. is thankful to University Grants Commission (WRO), Pune, India for providing the Teacher Fellowship under faculty improvement program.

References

[1] P. Nigam, G. Armour, I.M. Banat, D. Singh, R. Marchant, Physical removal of textile dyes from effluents and solid-state fermentation of dye-adsorbed agricultural residue, Bores. Tech. 72 (2000) 219-226.

[2] R. Ansari, Z. Mosayebzadeh, Removal of basic dye methylene blue from aqueous solutions using sawdust and sawdust coated with polypyrrole, J. Iran Chem. Soc. 7 (2010) 339-350.

[3] A. Khaled, P.N. Kapoor, K.J. Klabunde, Nanocrystalline metal oxides as new adsorbents for air purification, Nanostruct. Mater. 11(4) (1999) 459-468.

[4] Y.C. Sharma, V. Srivastava, S.N. Upadhay, C.H. Weng, Alumina nanoparticles for the removal of Ni (II) from aqueous solutions, Indus. Eng. Chem. Res. 47 (2008) 8095–8100.

[5] N. Varghese, M. Hariharan, A.B. Cherian, P.V. Sreenivasan, J. Paul, A. Antony, PVA - Assisted Synthesis and Characterization of Nano α –Alumina, Int. J. Sci. Res. Pub. 4(10) (2014) 1-5.

[6] Z. Zhang, T.M. Nenoff, K. Leung, S. Ferreira, J. Huang, et al., Room temperature synthesis of Ag-Ni and Pd-Ni alloy nanoparticles, J. Phys. Chem. C 114 (2010) 14309-14318.

[7] H. Hassena, Photocatalytic degradation of methylene blue by using Al_2O_3/Fe_2O_3 nano composite under visible light, Mod. Chem. Appl. 4 (2016) 176-1-5.

[8] M. Farahmandjou, N. Golabiyan, Solution combustion preparation of nano-Al_2O_3: synthesis and characterization, Trans. Phenom. Nano Micro Scale. 3(2) (2015) 100-105.

[9] M. Farahmandjou, N. Golabiyan, Synthesis and characterization of alumina (Al_2O_3) nanoparticles prepared by simple sol-gel method, Int. J. Bio-Inorg. Hybr. Nanomater. 5(1) (2016) 73-77.

[10] Y. Hyuk-Joon, W.J. Jin, T.K. Iu S.H. Kug, Temperature formation of α-alumina by doping of an alumina sol, J. Colloid Interf. Sci. 211(1) (1999) 110-113.

[11] M.R. Karim, M.A. Rahman, M.A.J. Miah, H. Ahmad, M. Yanagisawa, M. Ito, Synthesis of α-alumina particles and surface characterization, The Open Colloid Sci. J. 4 (2011) 32-36.

[12] H. Arami, M. Mazlomi, K. Khalifehzadeh, S.K. Sarnezhaad, Bundles of self-assembled boehmite nanostrips from a surfactant free hydrothermal route, J. Alloys Comp. 461 (2008) 551-554.

[13] S. Cava, S.M. Tebcherani, I.A. Souza, S.A. Pianaro, C.A. Paskocimas, et al., Structural characterization of phase transition of Al_2O_3 nanopowders obtained by polymeric precursor method, Materials Chem. Phy. 103 (2007) 394-399.

[14] R.J. Damani, P. Makroczy, Heat treatment induced phase and microstructural development in bulk plasma sprayed alumina, J. Eur. Ceram. Soc. 20 (2000) 867-888.

[15] C. Zuo, P.W. Jagodzinski, R-line luminescence from trace amounts of Cr^{3+} in aluminium oxide and its dependence on sample hydration, Appl. Spectrosc. 56 (2002) 1055-1058.

[16] A. Sedaghat, E. Taheri-Nassaj, R. Naghizadeh, An alumina mat with a nano microstructure prepared by centrifugal mathod, J. Non-Cryst. Solids 352(26-27) (2006) 2818-2828.

[17] P. Monash, G. Pugazhenthi, Removal of crystal violet dye from aqueous solution using calcined and uncalcined mixed clay adsorbents, Sep. Sci. Tech. 45(1) (2009) 94-104.

[18] Y.M. Zheng, N. Li, W.D. Zhang, Preparation of nanostructured microspheres of Zn-Mg-Al layered double hydroxides with high adsorption property, Colloids Surf. A: Physicochem. Engg. Aspects 415 (2012) 195-201.

[19] P. Monash, G. Pugazhenthi, Utilization of calcinied Ni-Al layered double hydroxide (LDH) as adsorbent for removal of methyl orange dye from aqueous solution, Environ. Prog. Sustain. Energy 33 (2014) 154-159.

[20] K. Byrappa, A.K. Subramani, S. Ananda, R.K.M. Lokanatha, R. Dinesh, Photocatalytic degradation of Rhodamine B dye using hydrothermally synthesized ZnO, Bull. Mater. Sci. 29 (2006) 433-438.

[21] J. Sun, L. Qiao, S. Sun, G. Wang, Photocatalytic degradation of Orange G on nitrogen – doped TiO_2 catalyst under visible light and sunlight irradiation, J. Hazard. Mater 155 (2008) 312–319.

[22] M. Huang, C. Xu, Z. Wu, Y. Huang, J. Lin, Photocatalytic discolouriazation of methyl orange solution by Pt modified TiO_2 loaded on natural zeolite, Dyes Pig. 77 (2008) 327-334.

[23] H.T. Lee, S. Wu, Assessment of the effect of azo dye Rp2B on the growth of nitrogen fixing cyanobacterium –*Anabena* Sp., Bioresource Technol. 77 (2001) 93-95.

https://doi.org/10.30799/jnst.192.19050101

Cite this Article as: Vijaya P. Dhawale, Datta J. Late, Satish D. Kulkarni, Synthesis, characterization of α-Al_2O_3 nanoparticles and its application in decolorization of methyl orange azo dye in the presence of UV light, J. Nanosci. Tech. 5(1) (2019) 580–583.